Diffusion of Propane in Zeolite NaY: A Molecular Dynamics and Quasi-Elastic Neutron Scattering Study

Ahmed Sayeed,[†] S. Mitra,[‡] A. V. Anil Kumar,[†] R. Mukhopadhyay,[‡] S. Yashonath,[†] and S. L. Chaplot*[,‡]

Solid State and Structural Chemistry Unit, Indian Institute of Science, Bangalore-560012, India, and Solid State Physics Division, Bhabha Atomic Research Centre, Trombay, Mumbai-400 085, India

Received: January 31, 2002; In Final Form: October 16, 2002

We report results from molecular dynamics (MD) simulations and quasi-elastic neutron scattering (QENS) measurements of the diffusion of propane in NaY zeolite at temperatures of 300, 324, and 350 K and a loading of 4 molecules per α-cage. The self-diffusivity, *D*, has been obtained from mean-squared displacement (msd), as well as from three different models of diffusion fitted to the intermediate scattering function ($F(Q,t)$) obtained from the MD simulation trajectories. All of the diffusivity values are consistent with each other. Further, these results are in good agreement with the experimental QENS results. It is found that the jump models describe both MD simulation and QENS data reasonably.

1. Introduction

Zeolites are porous crystalline materials that adsorb a number of molecules in relatively large quantities. This makes them useful in a number of industrial processes, mostly in petroleum and petrochemical industries, as catalysts and molecular sieves.[1−3] Hydrocarbons are separated and converted by the use of zeolites. For this reason, as well as for their intrinsic theoretical interest, the adsorption and transport of molecules, especially hydrocarbons, in zeolites are widely investigated experimentally and theoretically. During the past two decades, molecular dynamics (MD) simulations have provided a number of insights into the diffusion of guest molecules in zeolites. Among the experimental methods used for the study of self-diffusivity of hydrocarbons inside zeolite pores, quasi-elastic neutron scattering (QENS) and pulsed-field gradient NMR (PFG-NMR) are the most important. The results of these three methods of investigation—MD, QENS, and PFG-NMR—are generally found to be in good agreement for a number zeolite−sorbate systems.[2,4,6] Here, we present the results of our MD and QENS studies on the diffusion of propane in zeolite NaY. Preliminary QENS results have been reported in ref 7.

2. Methodology

2.1. Details of Molecular Dynamics Simulations. Molecular dynamics simulations of propane molecules confined to zeolite NaY have been carried out in the microcanonical ensemble. The simulation cell consists of one unit cell of zeolite NaY with 32 propane molecules at a loading of 4 molecules per supercage. Cubic periodic conditions are used in all three directions. Zeolite atoms are not included in the integration scheme. The rotational degrees of freedom are modeled using quarternion formalism.[8] Both translational and rotational equations are integrated using Gear predictor−corrector algorithm. An integration time step of 1 fs was found to be adequate to get good energy conservation. We have carried out three MD runs at temperatures of 300, 324, and 350 K. A production run of 1 ns duration has been used in obtaining averages after an initial equilibration period of 200 ps. The intermolecular potential parameters between propane and zeolite atoms are taken from the literature.[9,10] Lorentz−Berthelot combination rule is used to get the cross or mixed terms. The potentials are of the (6-12) Lennard-Jones form:

$$\phi(r) = 4\epsilon\left[\left(\frac{\sigma}{r}\right)^{12} - \left(\frac{\sigma}{r}\right)^{6}\right] \quad (1)$$

An all-atom model was used for propane, that is, the hydrogen-atom interactions are taken explicitly. The propane molecules were assumed to interact only with the oxygen atoms of the zeolite framework and with the extraframework cations. The Si and Al atoms in the zeolite host are well inside the framework and largely shielded by the surrounding oxygens, thus making the short-range interaction of these with the guest molecules insignificant. Hence, the interactions between Si and Al with oxygen atoms are not included. Table 1 lists the potential parameters for the propane−propane and propane−zeolite interactions.

TABLE 1: Potential Parameters for Propane−Propane and Propane−NaY Interactions

type	σ (Å)	ϵ (kJ/mol)
C−C	3.448	0.3874
H−H	2.980	0.0419
C−H	2.920	0.2054
C−O	2.996	0.7067
C−Na	3.409	0.1981
H−O	2.763	0.2324
H−Na	3.175	0.0405

2.2. Experimental Details. The NaY sample used had a Si/Al ratio ≈ 2.13 as determined by X-ray absorption spectroscopy. Accordingly, we have assumed a unit cell composition of $Na_{61}Al_{61}Si_{131}O_{384}$ for the purpose of calculating the mass of the unit cell. The sample X-ray diffraction (XRD) pattern shows good

[†] Indian Institute of Science.
[‡] Bhabha Atomic Research Centre.

10.1021/jp025576k CCC: $25.00
Published on Web 12/17/2002

crystallinity, and scanning electron microscopy (SEM) pictures show an average particle size of about 0.5 μm. The sample was first thoroughly dehydrated by evacuating for a period of about 12 h to 10^{-4} Pa at a temperature of 623 K. It was then transferred into two identical slab-shaped aluminum containers in ultra-high-pressure (UHP) nitrogen atmosphere. Each sample had dimensions of 6 cm in diameter and 0.5 cm in thickness. It was loaded with propane gas (purity > 99.9%) to saturation at ambient pressure. The loading was estimated gravimetrically to be 130 mg/g, which in this case turns out to be about 4.1 molecules per zeolitic supercage (α-cage). The maximum loading of propane was chosen to have enough intensity in the QENS experiment. The quantity of propane present in the sample was independently estimated also from neutron transmission measurements, and it was found to be very close to that of the loading amount.

The QENS experiments were performed using the quasi-elastic spectrometer[11] at Dhruva reactor at Trombay. The spectrometer is based on multiangle-reflecting-crystal (MARX) mode, for which one essentially uses a combination of a large crystal analyzer and a linear position-sensitive detector. In the present configuration, the spectrometer has an energy resolution of 200 μeV with an incident energy of 5.1 meV.[11,12] The quasi-elastic spectra were recorded in the wave vector transfer (Q) range of 0.67−1.8 Å^{-1} at 300, 324, and 350 K for both bare zeolite and zeolite with propane sample. The range of temperature over which we have carried out the measurements has been dictated by several considerations such as the experimental setup, stability of the zeolite, and restricted time scale over which the diffusion within the zeolite can be measured by QENS and MD. Spectra on a bare zeolite sample were recorded to estimate the contribution of bare zeolite to the total spectra.

3. Theory

3.1. Scattering Functions. In QENS experiments on a system of hydrocarbon molecules, the measured neutron intensity comes almost entirely from the incoherent scattering of neutrons from hydrogen atoms. This measured intensity, which is proportional to the double differential cross section of the hydrogen atom, is in turn proportional to the dynamical structure factor, $S(\mathbf{Q},\omega)$:[13]

$$\frac{\partial^2\sigma}{\partial\Omega\,\partial\omega} = \frac{k}{k_0}[\sigma_{\mathrm{inc}}^{\mathrm{H}} S(\mathbf{Q},\omega)] \tag{2}$$

where σ is the total scattering cross section, $\sigma_{\mathrm{inc}}^{\mathrm{H}}$ is the incoherent scattering cross section for hydrogen, $\mathbf{k}$ and $\mathbf{k}_0$ are the initial and final wave vectors with $\mathbf{Q} = \mathbf{k} - \mathbf{k}_0$, and ω is the angular frequency corresponding to energy transfer $\hbar\omega = E - E_0$. In the case of molecular diffusion, different kinds of motions—translational, rotational, and vibrational—take place simultaneously. It is generally assumed that these three motions are dynamically independent and can be analyzed separately. This is only an approximation, which is necessary for a mathematically tractable analysis. With this assumption, the total $S(\mathbf{Q},\omega)$, which is measured according to eq 2, can be expressed as a convolution product in ω of the different scattering functions.[13] In the quasi-elastic region (±2 meV), this can be written as

$$S_{\mathrm{inc}}(\mathbf{Q},\omega) = \exp(-\langle u^2\rangle Q^2)[S_{\mathrm{inc}}^{\mathrm{trans}}(\mathbf{Q},\omega) \otimes S_{\mathrm{inc}}^{\mathrm{rot}}(\mathbf{Q},\omega)] \tag{3}$$

The exponential term is the vibrational contribution, known as the Debye−Waller factor, where $\langle u^2\rangle$ is the mean-square displacement of the hydrogen atoms.

The dynamical structure factor, $S_{\mathrm{inc}}(\mathbf{Q},\omega)$, is related to the self-part of the intermediate scattering function, $F_{\mathrm{s}}(\mathbf{Q},t)$, through a Fourier transform:

$$S_{\mathrm{inc}}(\mathbf{Q},\omega) = \frac{1}{\pi}\int F_{\mathrm{s}}(\mathbf{Q},t)\exp(-i\omega t)\,\mathrm{d}t \tag{4}$$

The intermediate scattering function, $F_{\mathrm{s}}(\mathbf{Q},t)$, is a time-correlation function for a single particle and is defined by

$$F_{\mathrm{s}}(\mathbf{Q},t) = \langle \exp[i\mathbf{Q}\cdot(\mathbf{r}(t) - \mathbf{r}(0)]\rangle \tag{5}$$

where $\mathbf{r}(t)$ and $\mathbf{r}(0)$ are the position vectors of the scatterer (i.e., hydrogen) at time t and $t = 0$ and the angular brackets indicate ensemble average. Equation 3 can be expressed in terms of intermediate scattering functions for translational and rotational motions as follows (ignoring the vibrational term):

$$F_{\mathrm{s}}(\mathbf{Q},t) = F_{\mathrm{s}}^{\mathrm{trans}}(\mathbf{Q},t)\cdot F_{\mathrm{s}}^{\mathrm{rot}}(\mathbf{Q},t) \tag{6}$$

where

$$F_{\mathrm{s}}^{\mathrm{trans}}(\mathbf{Q},t) = \langle \exp[i\mathbf{Q}\cdot(\mathbf{R}(t) - \mathbf{R}(0))]\rangle \tag{7}$$

$$F_{\mathrm{s}}^{\mathrm{rot}}(\mathbf{Q},t) = \langle \exp[i\mathbf{Q}\cdot(\mathbf{d}(t) - \mathbf{d}(0))]\rangle \tag{8}$$

where $\mathbf{R}$ is the radius vector of the center of mass of a propane molecule in the fixed frame of reference and $\mathbf{d}$ is the radius vector of a hydrogen atom with respect to the center of mass of the propane molecule to which it belongs. It may be noted that $\mathbf{r} = \mathbf{R} + \mathbf{d}$. $S_{\mathrm{inc}}^{\mathrm{trans}}(\mathbf{Q},\omega)$ and $S_{\mathrm{inc}}^{\mathrm{rot}}(\mathbf{Q},\omega)$ can be obtained by taking the Fourier transforms of $F_{\mathrm{s}}^{\mathrm{trans}}$ and $F_{\mathrm{s}}^{\mathrm{rot}}$, respectively, as in eq 4.

As we shall discuss later, the experimental energy window used in this study effectively allows the observation of the translational motion only. This is because the rotational motion is relatively much faster and one needs to use a much wider energy window for its observation. The MD simulation results show that the rotational motion of the propane molecules is faster by an order of magnitude.

From the MD trajectories, we can readily calculate the intermediate scattering function for the molecular center of mass with

$$F_{\mathrm{s}}^{\mathrm{trans}}(\mathbf{Q},t) = \frac{1}{N}\sum_{i=1}^{N}\langle \exp[i\mathbf{Q}\cdot(\mathbf{R}_i(t+t_0) - \mathbf{R}_i(0))]\rangle \tag{9}$$

where $\mathbf{R}_i(t)$ is the position vector of the ith propane molecule at time t and N is the number of molecules used in the MD. The angular brackets denote (microcanonical) ensemble average, here an average over all of the initial times, t_0. The samples used in the QENS experiment were polycrystalline. Therefore, for the purpose of comparison of QENS and MD results, we have to take the powder average of eq 9:[14]

$$\langle F_{\mathrm{s}}(\mathbf{Q},t)\rangle = \frac{1}{N}\sum_{i=1}^{N}\left\langle \frac{\sin(|\mathbf{Q}||\mathbf{R}(t+t_0) - \mathbf{R}(t_0)|)}{|\mathbf{Q}||\mathbf{R}(t+t_0) - \mathbf{R}(t_0)|}\right\rangle \tag{10}$$

3.2. Diffusion Models. Various models are used in the study of self-diffusion of adsorbed molecules in zeolites. Often, use of some suitable model is necessary to calculate self-diffusivity from the experimental QENS results. The self-diffusivity values

can be calculated without resorting to any model, if QENS data can be obtained for sufficiently small Q values. This essentially corresponds to observing molecular motions over long distances, that is, over a number of unit cell distances. In this limit, molecular motion obeys Fick's law and the scattering function is a Lorentzian given by[13]

$$S_{\mathrm{inc}}^{\mathrm{trans}}(Q,\omega) = \frac{1}{\pi}\frac{DQ^2}{(DQ^2)^2 + \omega^2} \tag{11}$$

This Lorentzian has a half-width at half-maximum (hwhm) equal to DQ^2, so we can get D from the slope of a plot of hwhm vs Q^2, which should be a straight line. But in every real system, the diffusive motion begins deviating from Fickian form as the distances get shorter and shorter and the hwhm vs Q^2 plot is no longer a straight line for larger Q values. It is often possible to use some approximate model for short-range motion of the molecule as well, which can enable us to calculate D even with large Q data and at the same time give further valuable information about the diffusion mechanism.

For this purpose, different "jump diffusion models" have been used in a number of QENS studies of hydrocarbon diffusion in zeolites. We shall mention only three here, which we shall use in the analysis of our data. One is the so-called Chudley and Elliott (C−E) model, or the fixed jump-length model. In this model, molecular diffusion occurs though discrete jumps from one adsorption site to another, the length of jump remaining the same. If the jumps occur in random directions (i.e., isotropically), the hwhm, $\Gamma(Q)$, is given by[13,15]

$$\Gamma(Q) = \frac{1}{\tau}\left(1 - \frac{\sin Qd}{Qd}\right) \tag{12}$$

where τ is the time between two consecutive jumps (the residence time) and d is the jump length. The hwhm data from the QENS can be fitted to eq 12 with τ and d as adjustable parameters. The diffusion coefficient then can be calculated using the Einstein relation

$$D = \frac{d^2}{6\tau} \tag{13}$$

In another model attributed to Hall and Ross (H−R),[13,16] the jump distances make a Gaussian distribution and the scattering function, $S_{\mathrm{inc}}^{\mathrm{trans}}(Q,\omega)$, is a Lorentzian with hwhm given by

$$\Gamma(Q) = \frac{1}{\tau}\left[1 - \exp\left(-\frac{Q^2\langle d^2\rangle}{6}\right)\right] \tag{14}$$

Here, τ is the residence time and $\langle d^2\rangle^{1/2}$ is the root-mean-square jump length. D can be calculated from eq 13 as in the first case. It can be easily shown that in the limit of small Q both jump models, given by eqs 12 and 14, have the same asymptotic behavior as the Fickian model, that is, hwhm is proportional to Q^2.

The third model is attributed to Jobic.[17] It is an extension of the above fixed jump-length model. Here, the molecule is assumed to jump from one adsorption site to another but is supposed to be "delocalized" at the adsorption site over a certain delocalization length. The jump-length distribution is given by

$$\rho(r) = \frac{r}{\sqrt{2\pi}dr_0}\exp\left[-\frac{(r-d)^2}{2r_0^{\,2}}\right] \tag{15}$$

where r is the jump distance, d is the distance between two sites, and r_0 is the delocalization length. The mean-square jump length is given by

$$\langle r^2\rangle = \int_0^\infty r^2\rho(r)\,\mathrm{d}r = d^2 + 3r_0^{\,2} \tag{16}$$

and the expression for the hwhm is

$$\Gamma(Q) = \frac{1}{\tau}\left[1 - \left(\frac{(\sin Qd)}{Qd}\right)\exp\left(-\frac{Q^2r_0^{\,2}}{2}\right)\right] \tag{17}$$

This model takes into account to some extent the well-known fact that the molecules do not remain fixed on an adsorption site between jumps but rather oscillate and hover around it, unless the temperature is very low. Near room temperature, this kind of delocalization is generally expected.

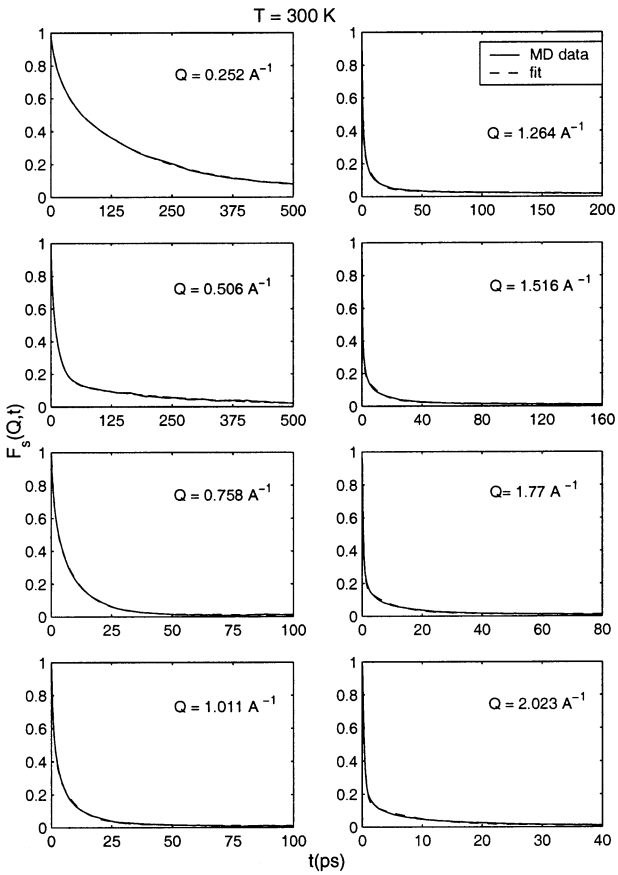

Figure 1. The $F_s(Q,t)$ vs t plot at eight different Q values from 0.2528 through 2.022 Å^{-1} in increments of 0.2528 Å^{-1} at 324 K. The dashed line shows the fit of eq 18.

4. Results and Discussion

4.1. MD Simulation. In this study, we are mainly concerned with comparing MD and QENS results. Because we directly calculate $F_s(Q,t)$ from the MD data using eq 10, it is preferable to work with this function itself rather than its Fourier transform (eq 4) in the frequency domain. The typical $F_s(Q,t)$ vs t plots at $T = 300$ K are presented in Figure 1. The $F_s(Q,t)$ is calculated at eight different Q values from 0.2528 through 2.022 Å^{-1} in increments of 0.2528 Å^{-1}. This is the smallest value of Q that can be used in the present MD study because of the requirement that each Cartesian component of Q must be an integral multiple of $2\pi/L$, L being the length of the cubic simulation box. This requirement arises as a consequence of the periodic boundary conditions used for the simulation.[18]

In section 3.2, we discussed three commonly used diffusion models, all of which yield a Lorentzian form for $S_{inc}(Q,\omega)$ vs ω plots with hwhm $\Gamma(Q)$. In the time domain, this is equivalent to an exponential form, $F_s(Q,t) \propto \exp(-\Gamma(Q)t)$. But we find that a single exponential does not give a very good fit to $F_s(Q,t)$ vs Q obtained from the MD simulations. This is observed quite generally in the MD studies of diffusion in a number of systems, that is, the $F_s(Q,t)$ cannot be modeled over the entire time range under consideration with a single exponential.[19] In such a situation, usually a linear sum of a number of exponentials or a combination of exponentials and Gaussians is considered. For instance, Trouw[18] in his MD study of methane in ZSM-5 fits $F_s(Q,t)$ to a sum of a Gaussian (for fast decay) and an exponential (for slow decay). And Cola et al.[20] in their MD study of supercooled water use a sum of three exponentials. It is sometimes possible to interpret each component as representing a particular mode of diffusion, as we shall discuss below.

We have considered different alternatives with a combination of Gaussians and exponentials to model our $F_s(Q,t)$ vs t data. We found that a linear sum of three exponentials gives a reasonably good fit over the entire t and Q range and is better than other alternatives such as a Gaussian and two exponentials. So, the model that we have used is given by

$$F_s(Q,t) = C_1(Q)\, e^{-\Gamma_1(Q)t} + C_2(Q)\, e^{-\Gamma_2(Q)t} + C_3(Q)\, e^{-\Gamma_3(Q)t} \quad (18)$$

The first exponential describes the fast diffusion component, the second the intermediate component, and the third the slow component. The $C(Q)$'s and $\Gamma(Q)$'s are the fitting parameters.

The MD data, together with fits, are shown in Figure 1 typically for $T = 324$ K. We can see that the fits are reasonably good for the entire ranges of t and Q. Figure 2 shows the three components for each Q value at the temperature 324 K. The components are similar for the other two temperatures. The decay constants for these components were obtained at different temperatures. The values of $1/\Gamma_1(Q)$, $1/\Gamma_2(Q)$, and $1/\Gamma_3(Q)$ are in the range of $\sim$0.3−7, $\sim$7−70, and $\sim$70−700 ps, respectively. The intermediate component matches with the one observed in the QENS experiment. Variation of decay constant $\Gamma_2(Q)$ with Q^2 is shown in Figure 3. This is the component that is mainly responsible for the diffusive motion of the propane molecules. The characteristic decay time $1/\Gamma_1(Q)$ (below 6 ps) describes short-range rapid motion and does not contribute much to proper long time limit diffusion of the molecule. Physically, this might be the motion of shuttling and rattling of molecules at an adsorption site, quite commonly observed in the case of molecules adsorbed in zeolite.[17] The third component $\Gamma_3(Q)$ mainly accounts for long time tail of $F_s(Q,t)$ above 60 ps. Physically speaking, we obtain this slow component because of molecules that remain pratically immobile over the time scale of observation. For example, Jobic et al.[5] have observed this kind of relative immobility on the time scale of their experiment for xylenes in X-type zeolites.

The Q dependence of $\Gamma_2(Q)$ (Figure 3) shows a typical jump diffusion character with an initial rapid increase and then a saturation at higher Q values. We have tried to fit all of the three models described in section 3.2. As far as the overall goodness of fit is concerned, all three give more or less equally good fit. While the Chudley and Elliott model shows oscillatory behavior with Q, such behavior is not found in H−R and Jobic models. Further, while the coefficients obtained for the Jobic model are realistic and seem reasonable, the error indicated on individual parameters by the fitting algorithm is found to be large. The values of diffusivity D, jump length d, and residence time τ from these three models are presented in Table 2. The values of delocalization length r_0 in the Jobic model, as well as D values from mean-squared displacement (msd) vs time plots, are also given. The D values calculated from msd vs time data, which are independent of any model, show a small increase with temperature, from 1.32×10^{-9} to 2×10^{-9} m^2/s, as expected. Figure 4 shows msd vs time plots for the three temperatures.

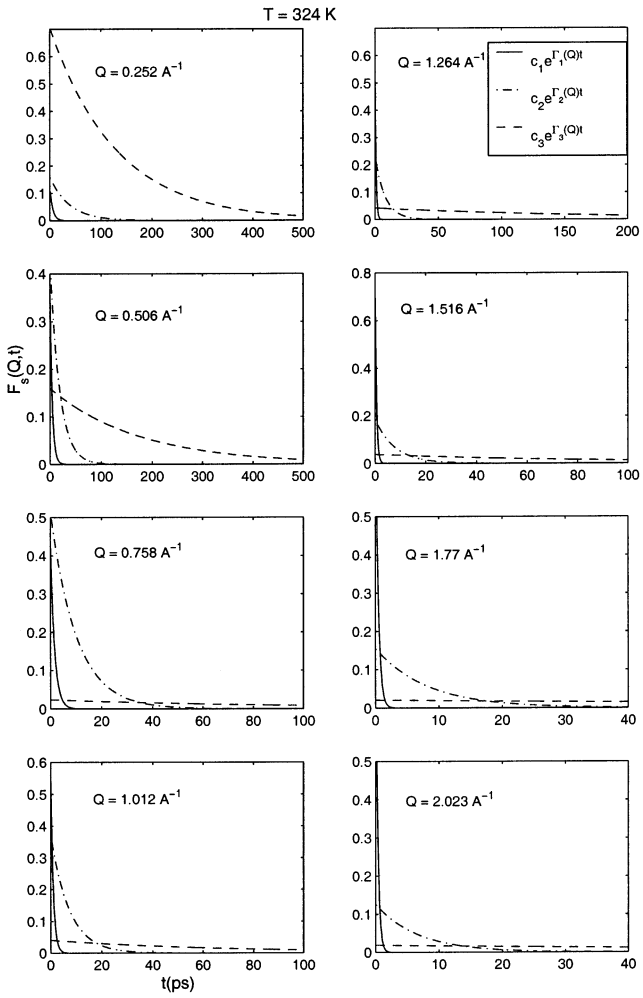

Figure 2. The plots showing the three components in eq 18 separately for different Q values at 324 K.

We cannot attach any significance to the small apparent variations in the D values (Table 2) at different temperatures because the variation is within the error bars. The values obtained from model calculations, $\sim 3 \times 10^{-9}$ m^2/s, are of the same order as the values obtained from msd vs time plots, $\sim 1.5 \times 10^{-9}$ m^2/s, which is a good agreement. The jump distances obtained are $\sim$4 Å. We have calculated the average distance between adsorption sites by carrying out an MD run at 10 K. At this temperature, the particles will be essentially trapped in the adsorption site with very little delocalization. Then the analysis of the MD trajectory will give the positions of the adsorption sites. The average distance between the neighboring adsorption sites is 5.7 Å. At higher temperatures, there is delocalization of particles in the immediate neighborhood of the adsorption sites, and this will reduce the distance between the adsorption sites. So, we can naturally identify this jump diffusion as the jumps between two adsorption sites. As we are going to discuss later, these diffusivity and jump distance values compare well with experimental values.

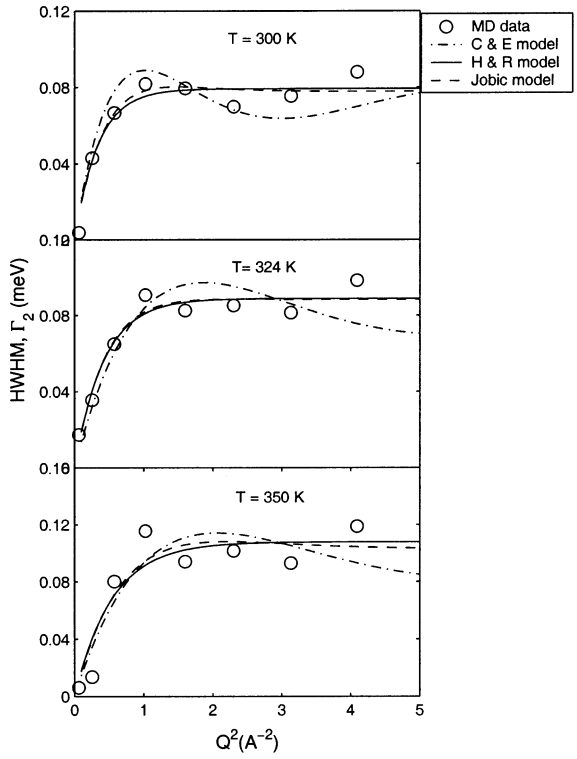

Figure 3. The Q dependence of Γ_2, showing a typical jump diffusion at three different temperatures, 300, 324, and 350 K. The ○ shows the points obtained from MD simulations. The curves are the fits of different models to the data; the continuous line represents the Hall and Ross model; the dotted line represents the Chudley and Elliot model; the dashed line represents the Jobic model).

TABLE 2: Average Dynamical Properties Obtained from MD Simulations and QENS Experiment[a]

		MD simulation study				QENS experiment		
T (K)	parameter	H−R	C−E	Jobic	msd	H−R	C−E	Jobic
300	D ($\times 10^{-9}$ m^2/s)	3.6	3.7	2.0	1.32	2.3	2.0	1.3
	d (Å)	4.2	4.5	3.2		2.5	2.7	2.0
	τ (ps)	8.3	9.0	8.5		4.6	5.9	4.9
	r_0 (Å)			1.5				0.9
324	D ($\times 10^{-9}$ m^2/s)	3.2	2.2	1.2	1.9	3.2	2.7	0.5
	d (Å)	3.8	3.3	2.3		2.9	2.9	1.2
	τ (ps)	7.4	8.2	7.4		4.3	5.3	4.3
	r_0 (Å)			1.7				1.5
350	D ($\times 10^{-9}$ m^2/s)	3.0	2.3	1.8	2.0	4.0	3.2	0.7
	d (Å)	3.3	3.1	2.6		3.0	3.0	1.3
	τ (ps)	6.1	7.0	6.4		3.8	4.7	3.8
	r_0 (Å)			1.2				1.6

[a] H−R denotes Hall−Ross model; C−E denotes Chudley−Elliot model; Jobic denotes Jobic model; msd denotes mean-square displacement. The standard errors in the QENS experimental value of D are $\pm 0.3 \times 10^{-9}$ m^2/s for H−R and C−E models and $\pm 1.5 \times 10^{-9}$ m^2/s for the Jobic model.

4.2. Experimental Results. We observed that the bare, dehydrated zeolite sample did not show any quasi-elastic (QE) broadening, whereas propane-loaded sample did show significant QE broadening even at room temperature, indicating presence of dynamical motion of propane molecules. At the first instant, the elastic and quasi-elastic components in the total spectrum were separated. The data analysis involves convolution of the model scattering function, $S(Q,\omega)$, written as

$$S(Q,\omega) \propto [A(Q)\delta(\omega) + [1 - A(Q)]L(Q,\omega)] \qquad (19)$$

with the instrumental resolution function, which was obtained by measuring spectra from a standard vanadium sample. The first term in the above equation is the elastic part, and the second is the quasi-elastic one. $L(Q,\omega)$ is a Lorentzian with hwhm Γ. The dynamical parameters ($A(Q)$ and Γ) were obtained by least-squares fit. It was found that there was no extraelastic component other than that present in the bare zeolite itself. The separated elastic and QE components at different Q values typically at $T = 324$ K are shown in Figure 5. It is found that a single Lorentzian could describe the QE part very well suggesting that only the translational motion is contributing to the observed data. This is consistent with our MD simulation in which it was found that propane undergoes very fast rotational motion in the cages of NaY zeolite, which is beyond the range observable with the present energy window of our spectrometer. This fact is also illustrated in the MD snapshots of a propane shown in Figure 6. Here, it can be clearly seen that when the molecule has rotated by about π radians, the center of mass itself has hardly moved. The estimated widths of rotational spectra from the MD run were found to be ~30 times higher than those of translational ones. Therefore, the rotational motion will not make observable contribution to the experimental data in the present experimental set up, which is designed to investigate dynamics in the time scale of ~10 ps. However, we plan to carry out a QENS experiment with a suitably large energy window on another neutron spectrometer at Trombay to estimate the contribution of rotational motion as indicated by the MD simulation study.

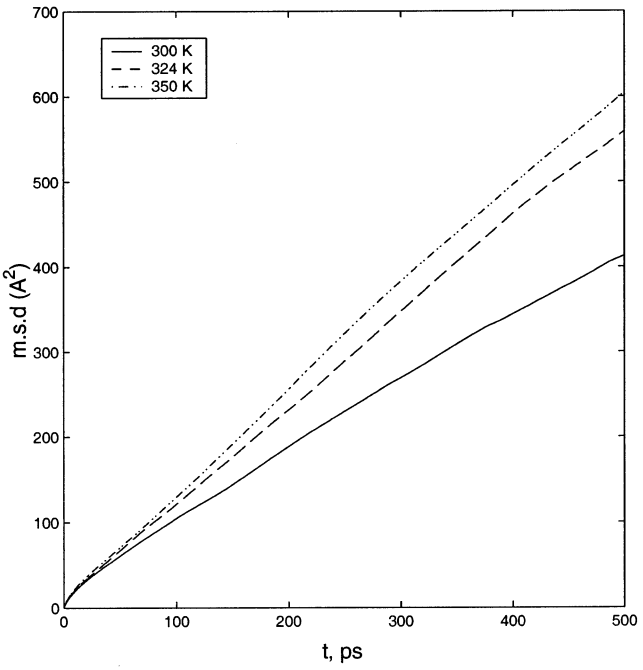

Figure 4. Mean-square displacement vs time plots obtained from MD simulations at 300, 324, and 350 K.

The hwhm vs Q^2 plots for the three temperatures are shown in Figure 7. All of the models described in section 3.2 have been fitted to the data. Both H−R and Jobic models describe the QENS data equally well. However, surprisingly, the errors associated with the fitted parameters in the Jobic model are larger despite the larger number of parameters that it involves. The experimental data do not really show the oscillatory variations expected in the C−E model. The dynamical parameters as obtained from the fit with the three different models are given in Table 2. We see that these numbers are in good agreement with the values obtained from MD results. Also, these

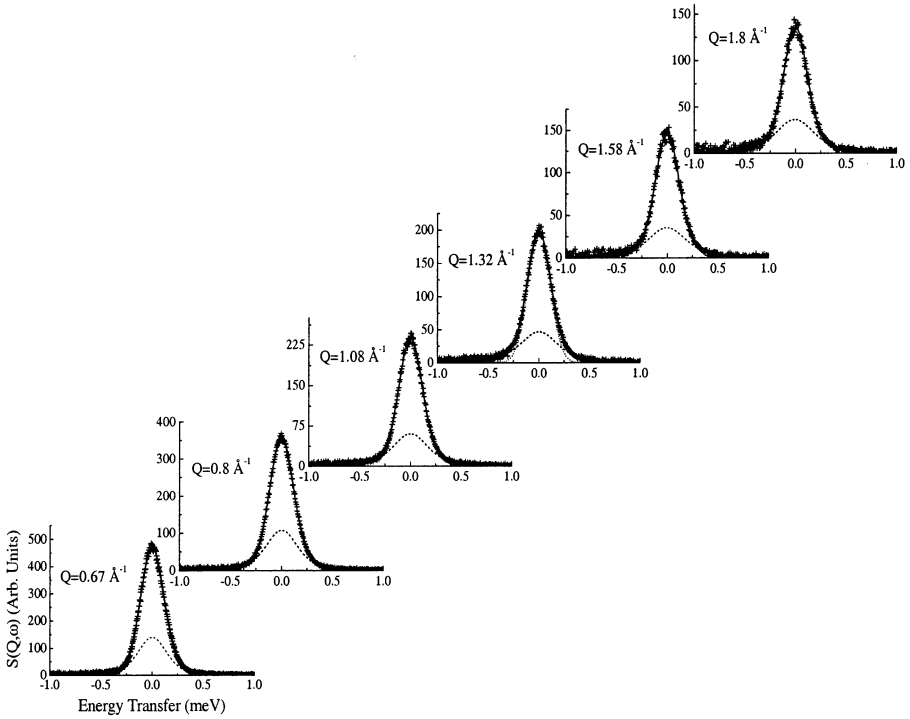

Figure 5. $S_{inc}^{trans}(Q,\omega)$ at different Q values obtained from the QENS experiment at $T = 324$ K.

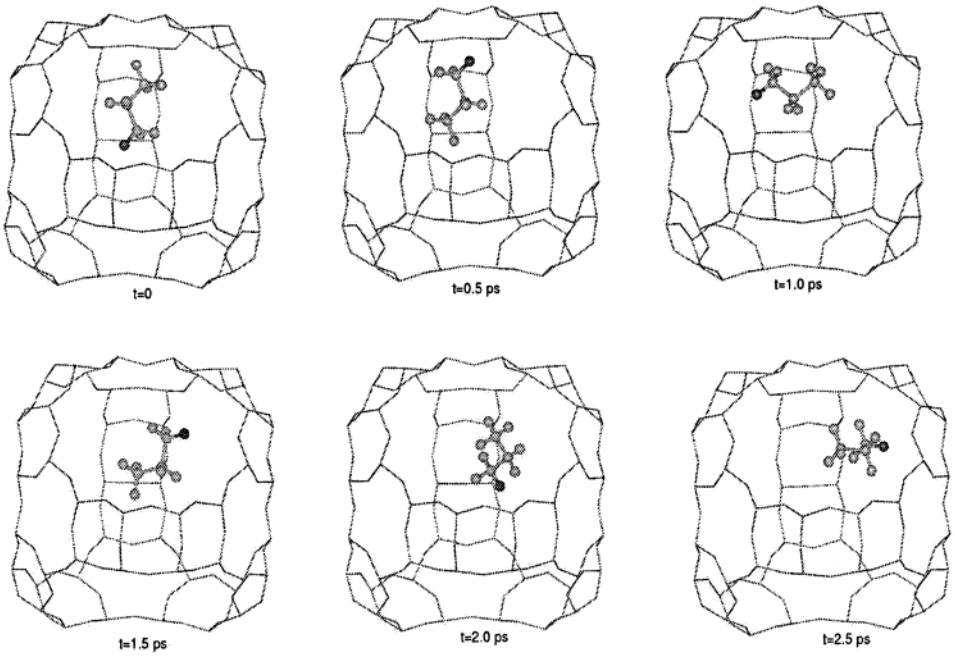

Figure 6. Snapshots from molecular dynamics to show the translational and rotational motion. A single hydrogen of the CH_3 group in propane is shown darker to distinguish it from others to be able to recognize rotation when it occurs. Rotation through an angle π can be seen within 0.5 ps. During this period, little or no translation is seen.

are comparable to the D values obtained from the PFG-NMR studies of propane diffusion NaX, which is a similar system.[21]

5. Conclusions

We have carried out MD simulations and QENS measurements on the diffusion of propane in zeolite NaY with a loading of 4 molecules per cage at three temperatures (300, 324, and 350 K). Calculation of the self-diffusivity, D, is carried out from the simulated mean-squared displacement, as well as from three different models of diffusion fitted to the intermediate scattering function. From MD, it is found that the translational motion of the propane molecules occurs at three different time scales. The hwhm for the intermediate times, Γ_2, vs Q^2 is well described by the Gaussian jump model. The self-diffusivities, residence times, and jump lengths obtained from the QENS studies are in reasonable agreement with those obtained from MD. The largest deviation is of τ, which is significantly higher for the MD as compared to the QENS. This suggests that the intermolecular potential for the guest−host, as used in the MD simulation, is stronger than what the experiments suggest. The Lennard-Jones parameter ϵ between the carbon and hydrogen and the oxygen of the zeolite needs to be reduced. With reduced

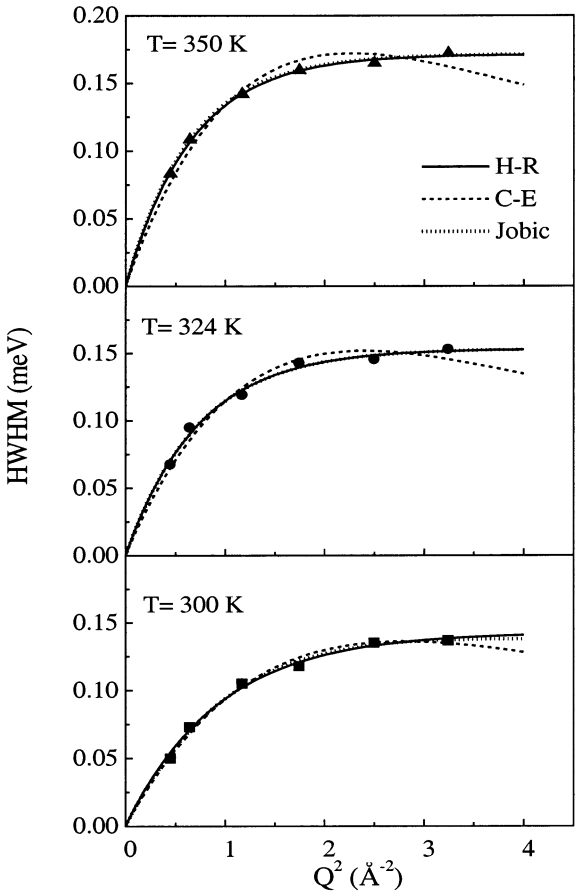

Figure 7. The Q dependence of hwhm of the Lorentzian function, $\Gamma(Q)$, obtained from the experimental QENS data fitted with different model functions (see text).

guest−host interaction strength in the MD simulation, the propane molecules would spend less time in the adsorption site and consequently a Gaussian distribution of jumps would be more appropriate. More careful simulations and neutron measurements over a larger temperature range might be helpful to discriminate among the different models. However, over all there is reasonable agreement between MD and QENS results, and this is encouraging.

Acknowledgment. Authors thank IUC-DAEF for support in carrying out this work. We also thank Professor M. S. Hegde for providing laboratory facilities. We also thank DST, New Delhi, for financial support for computational facilities through a grant.

Supporting Information Available: Values of C and Q parameters obtained by fitting eq 18 to the $F_s(Q,t)$ obtained from MD simulations. This material is available free of charge via the Internet at http://pubs.acs.org.

References and Notes

(1) Barrer, R. M. *Zeolites and Clay Minerals*; Academic Press: London, 1978.

(2) Kärger, J.; Ruthven, D. M. *Diffusion in Zeolites and Other Microporous Solids*; Wiley-Interscience: New York, 1992.

(3) Bates, S. P.; van Santen, R. A. *Adv. Catal.* **1997**, *42*, 1.

(4) Jobic, H.; Bee, M.; Kearly, G. J. *J. Phys. Chem.* **1994**, *98*, 4660.

(5) Jobic, H.: Bee, M.; Frick, B.; Methivier, A. *Proc. Int. Zeolite Conf., 12th* **1994**, 59.

(6) Snurr, R. Q.; Kärger, J. *J. Phys. Chem. B* **1997**, *101*, 6469.

(7) Mitra, S.; Mukhopadhyay, R.; Sayeed, A.; Yashonath, S.; Chaplot, S. L.; *Appl. Phys. A*, in press.

(8) Evans, D. J. *Mol. Phys.* **1977**, *34*, 317.

(9) Filippini, G.; Gavazzotti, A. *Acta Crystallogr. B* **1993**, *49*, 868.

(10) Santikary, P.; Yashonath, S. *J. Chem. Soc., Faraday Trans.* **1992**, *88*, 1063.

(11) Mukhopadhyaya, R.; Mitra, S.; Paranjpe, S. K.; Dasannacharya, B. A. *Nucl. Instrum. Methods Phys. Res., Sect. A* **2001**, *474*, 55.

(12) Dasannacharya, B. A. *Physica B* **1992**, *180a and 181*, 880.

(13) Bee, M. *Quasielastic Neutron Scattering*; Adam Hilger: Bristol, U.K., 1988.

(14) Herwig, K. W.; Wu, Z.; Dai, P.; Taub, H.; Hansen, F. Y. *J. Chem. Phys.* **1997**, *107*, 5186.

(15) Chudley, C. T.; Elliott, R. J. *Proc. Phys. Soc. London* **1961**, *77*, 353.

(16) Hall, P. L.; Ross, D. K. *Mol. Phys.* **1981**, *42*, 673.

(17) Gergidis, L. N.; Theodorou, D. N.; Jobic, H. *J. Phys. Chem. B* **2000**, *104*, 5541.

(18) Trouw, F. R. *Spectrochim. Acta* **1992**, *48A*, 455.

(19) Balucani, U.; Zoppi, Z. *Dynamics of Liquid State*; Clarendon: Oxford, U.K., 1994.

(20) Cola, D. D.; Sampoli, M.; Torcini, A. *J. Chem. Phys.* **1996**, *104*, 4223.

(21) Caro, J.; Bulow, M.; Schimer, W.; Kärger, J.; Heink, W.; Pfeifer, H.; Zdanov, S. P. *J. Chem. Soc., Faraday Trans. I* **1985**, *81*, 2541.